IR LED Calibration Sources for Space Applications

John Silny, Cherizar Walker, Jason Smith
Systems Development Center
Raytheon Space and Airborne Systems
El Segundo, CA, USA
jsilny@raytheon.com, cherizar_walker@raytheon.com, jason_a_smith@raytheon.com

Abstract – *Infrared (IR) light emitting diodes (LEDs) are evaluated as a viable replacement for existing space calibration sources. The diodes, that are of varying nominal center wavelengths, are characterized in two phases: 1) optical performance at cryogenic temperatures and 2) performance degradation due to total ionizing dose radiation exposure. Test data demonstrates that at cryogenic temperatures the diodes are up to 20 times more efficient than at room temperature and only require 60% more electrical input power. They are spatially uniform and radiometrically stable over long operational periods. Testing has also determined that certain LEDs exhibit no significant changes when exposed to radiation. In summary, test data indicates that IR LEDs are well suited as calibration sources for space applications.*

Keywords: light emitting diode, calibration source, non-uniformity correction, total ionizing dose radiation testing.

1 Introduction

Infrared (IR) space-borne sensors make use of internal calibration sources for generation of flat field calibration coefficients used to correct pixel-to-pixel non-uniformities in detector response [1]. Historically, these calibration sources have generally consisted of tungsten filament style lamps or blackbody emitters. Each of these sources presents a number of integration and performance challenges. For example, tungsten filament sources must operate without a glass envelope to be used in the infrared spectral region, exposing the sensor to potential contamination from hot tungsten sputter. Furthermore, such sources can only be operated in a vacuum which complicates ground testing. Lamp filaments also have a very limited calibration lifetime, with a trade between source brightness, color temperature, and total number of operational hours. Blackbody calibration sources are typically large and heavy, requiring substantial power to operate. Blackbodies emit at a lower operating temperature than filament lamps, and therefore require a much larger emitter area to achieve similar flux levels. Both lamp filament and blackbody sources present challenges to IR sensor thermal design due to their broad spectral output, high power consumption, relatively low efficiency, and long warm up times typically needed to meet radiometric stability requirements.

Recently, infrared light emitting diode (LED) sources have been developed that may provide a solution to a number of the issues related to tungsten lamp and blackbody sources. LEDs, ubiquitous for use in indicators, make use of solid state semiconductors for light generation. They are spectrally efficient, emitting light in limited, although selectable, wavelength bands, and may produce more uniform illumination than tungsten lamps since they do not make use of a filament. They can be turned on and off at high temporal rates, and may not require warm-up time for repeatable operation. In short, LED calibration sources may provide a number of advantages over traditional IR calibration sources. However, LEDs have not been widely used in space sensors, so they require evaluation of optical characteristics as well as long-term survivability in a space environment.

The idea of using LEDs for space-based sensor calibration is not novel. For example, in 1998 Starikov *et al.* considered using ultraviolet, visible, and near IR diodes for calibration of an on-orbit sensor [2]. Their paper analyzes the band-gap structure of various materials and the relative output spectrum vs. wavelength of such devices. In 2000, Nieke *et al.* proposed using visible and near IR LEDs to calibrate a space-borne spectrometer [3]. Their paper presents a detailed optical characterization of center wavelength, spectral bandwidth, and changes in these parameters with temperature and operating current for a set of units under test. The authors even go so far as to model the effects of space radiation on the LED materials. However, to the best of our knowledge, this paper is the first in two areas: (1) to present the idea of using mid-wave infrared (MWIR) LEDs as on-orbit calibration sources with supporting optical property characterization data, and (2) to present test data demonstrating the optical stability of such devices when exposed to total ionizing dose radiation similar to that within a space environment.

2 Objectives

IR LED sources are evaluated as replacements for tungsten lamp and blackbody emitter sources. A set of IR LEDs was selected for operation in the MWIR spectral band between 3 and 5 microns of wavelength. The LEDs are characterized over a range of cryogenic operating temperatures typically used in IR sensor applications.

Performance evaluations are performed in two phases. The first phase focuses on measuring the optical properties of the light sources as a function of operating temperature, including power efficiency, brightness, spectral composition, stability, and illumination uniformity. The second phase evaluates performance degradations due to total ionizing dose (TID) exposure similar to that experienced in a space environment.

3 Approach

Four IR LED sources with lenses and nominal center wavelengths of 3.4, 3.6, 3.8, and 5.4 μm are procured and characterized in two phases. The first phase evaluates the following characteristics:

- Spectral center wavelength versus temperature
- Spectral bandwidth versus temperature
- Electrical operating power versus temperature
- Absolute spectral irradiance versus temperature
- Irradiance spatial distribution uniformity
- Relative output intensity versus angle of incidence
- Lens survivability at cryogenic temperatures
- Radiometric stability over continuous operation.

Characterization measurements are performed at cryogenic temperatures (130, 140, and 150 K) and at room temperature (297 K). For cryogenic operation, the LEDs are mounted in a liquid nitrogen dewar equipped with an IR window of known spectral transmittance. The dewar is instrumented with a heater, temperature sensor, and closed loop proportional-integral-derivative (PID) controller to accurately regulate the operating temperature. The LED spectral characteristics are measured using a scanning monochromator with diffraction grating and IR point detector. The spatial and radiometric characteristics of the LED are measured using an IR camera as an imaging radiometer. The camera and the monochromator detector are radiometrically calibrated using a cavity blackbody radiator as a standard of spectral radiance. Measurements with the two test configurations are combined to measure the absolute spectral irradiance of the LEDs. Stability of the LEDs is monitored over multiple hours of continuous operation The electrical operating characteristics are recorded directly from the LED constant current drive electronics and measurements of the forward voltage drop over temperature. The survivability of the LED lenses is evaluated after more than 10 thermal cycles between ambient temperature and 77 K.

The second phase of testing evaluated how the optical properties of the LEDs degraded with TID radiation exposure, including:

- Relative radiometric output versus exposure level
- Relative spectral irradiance versus exposure level
- Spatial uniformity versus exposure level.

The LEDs under test are irradiated using a metered radioactive source with calibrated dosimeters in an enclosed chamber. The exposures are carefully calibrated to include geometric effects such a $1/R^2$ irradiance fall-off and multiple reflections within the chamber. Additionally, the LEDs are kept at cryogenic temperature in a non-powered state during exposure to maintain any temperature dependent radiation changes. Radiometric and spectral characteristics are monitored using the same camera and monochromator test configurations as in the first phase.

4 Results

The LED characterization results are divided into two sections, one for each phase of the project.

4.1 Phase One Results

The relative spectral irradiance of each LED at normal exitance and as a function of temperature is measured using the scanning monochromator with a spectrally flat fielded detector. The center wavelength (corresponding to peak spectral irradiance) and the spectral bandwidth (computed as a full width at half maximum, FWHM) are numerically extracted from the relative irradiance curves. Tables 1 and 2 summarize the spectral center and bandwidth properties for each LED over temperature. Observe that the spectral centers shift to shorter wavelengths and the spectral bandwidths narrow as the operating temperatures are decreased. Table 3 shows the input electrical power (excluding the forward voltage) required to operate each LED with a constant current of 193 mA. The increase in power at colder temperatures is due to an increase in source voltage to maintain constant current.

Table 1. LED Spectral Center. Values are reported in units of μm with a maximum uncertainty of ±0.003 μm (1σ).

		Operating Temperature (K)			
		130	140	150	297
LED Unit Under Test	3.4 μm	2.996	3.014	3.037	3.409
	3.6 μm	3.239	3.255	3.274	3.645
	3.8 μm	3.403	3.420	3.441	3.814
	5.4 μm	4.553	4.590	4.630	5.437

Table 2. LED Spectral Bandwidth. Values are reported in units of nm with a maximum uncertainty of ±3 nm (1σ).

		Operating Temperature (K)			
		130	140	150	297
LED Unit Under Test	3.4 μm	284	293	302	390
	3.6 μm	365	374	387	432
	3.8 μm	314	324	335	423
	5.4 μm	296	315	349	512

Table 3. LED Input Electrical Power. Values are reported in units of mW with a maximum uncertainty of ±2 mW (1σ).

		Operating Temperature (K)			
		130	140	150	297
LED Unit Under Test	3.4 µm	90	89	87	63
	3.6 µm	74	74	72	48
	3.8 µm	69	68	67	44
	5.4 µm	58	57	56	33

Figure 1 plots the spectral irradiance at normal exitance vs. wavelength at multiple operating temperatures for LED 3.6 as measured by the scanning monochromator and calibrated to absolute radiometric units at a distance of 92 mm. The curves show a dramatic increase in the total radiometric output and a shift to shorter wavelengths from ambient to cryogenic temperature.

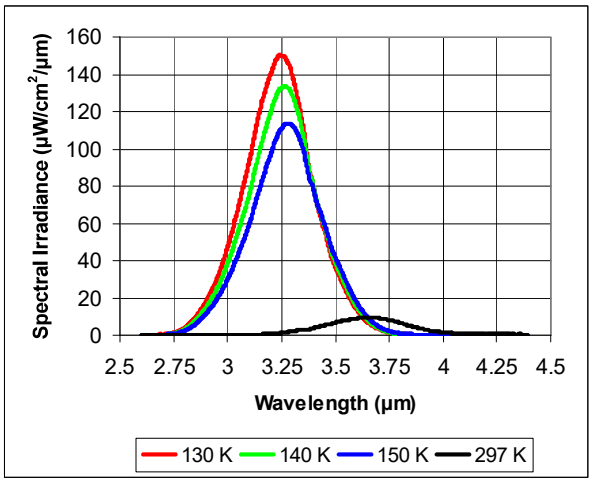

Figure 1. Absolute spectral irradiance as a function of operating temperature for LED 3.6 at a distance of 92 mm.

Table 4 summarizes the peak spectral irradiance for each LED as a function of operating temperature. The peak spectral irradiance increases by up to a factor of 23 at cryogenic temperatures while only drawing approximately 60% more electrical input power.

Table 4. LED Spectral Irradiance at Normal Exitance. Values are reported in units of µW/cm²/µm at a distance of 92 mm with a maximum uncertainty of ±6% (1σ).

		Operating Temperature (K)			
		130	140	150	297
LED Unit Under Test	3.4 µm	1130	809	640	57.6
	3.6 µm	150	134	113	9.56
	3.8 µm	71.9	59.4	41.8	3.12
	5.4 µm	6.32	4.86	3.61	0.268

The spectral irradiance distributions of all tested LEDs are well approximated (root mean square error, RMSE < 2% for all fits) by a Gaussian function of the form[1]

$$E_\lambda = a \exp\left[-4\ln(2)\left(\frac{\lambda - b}{w}\right)^2\right] \qquad (1)$$

in which a is the peak spectral irradiance (Table 4), b is the spectral center (Table 1), w is the FWHM spectral bandwidth (Table 2), λ is the wavelength, and $\ln(x)$ is the natural logarithm function. The irradiance can then be computed by the following spectral integral

$$E = \int_{-\infty}^{\infty} E_\lambda d\lambda = aw\tfrac{1}{2}\sqrt{\pi/\ln(2)} \qquad (2)$$

Such a mathematical representation is quite useful for radiometric modeling purposes.

The spectrally averaged quantum efficiency (QE) of each LED at temperature T can be computed as

$$\eta(T) = \frac{\int\int E_{\lambda,T} \frac{\lambda}{hc} d\lambda dA}{i/q} \quad \frac{[\text{ph/s}]}{[\text{e}^-/\text{s}]} \qquad (3)$$

in which $E_{\lambda,T}$ is the spectral irradiance at temperature T, λ/hc is the number of photons per unit energy, c is the speed of light, h is Planck's constant, i is the input electrical current, and q is the elementary charge of an electron. To accurately measure the QE in absolute units, the irradiance would need to be sampled and integrated over a full hemisphere. Alternatively, the relative increase in QE between two temperatures can be more easily measured by computing the unitless ratio[2]

$$R_{21} = \frac{\eta(T_2)}{\eta(T_1)} = \frac{\int\int E_{\lambda,T_2} \frac{\lambda}{hc} d\lambda dA}{\int\int E_{\lambda,T_1} \frac{\lambda}{hc} d\lambda dA} \qquad (4)$$

If the spatial distribution of irradiance is assumed to be invariant with changes in temperature (a reasonable assumption), then Equation 4 can be simplified as

$$R_{21} = \frac{\int E_{\lambda,T_2} \lambda d\lambda}{\int E_{\lambda,T_1} \lambda d\lambda} \qquad (5)$$

[1] The factor –4 ln(2) in Eq. (1) forces w to be a FWHM, whereas a value of –1/2 would make w a 1σ width parameter.

[2] The ratio of input electrical currents is equal to unity since the LEDs are operated in a constant current mode.

which is simply the ratio of spectral irradiance centroids. Table 5 summarizes the relative increase in QE over temperature as computed using Equation 5. The ratios are normalized to a value of 1.00 at 130 K. Increases in quantum efficiency as large as 20 to 1 are realized under cryogenic operating conditions.

Table 5. LED Relative Quantum Efficiency. Values are normalized ratios with a maximum uncertainty of ±9% (1σ).

		Operating Temperature (K)			
		130	140	150	297
LED Unit Under Test	3.4 µm	1.00	0.74	0.61	0.10
	3.6 µm	1.00	0.90	0.80	0.09
	3.8 µm	1.00	0.86	0.64	0.06
	5.4 µm	1.00	0.73	0.54	0.05

Figure 2 displays a two-dimensional spatial distribution of the absolute irradiance at a distance of 92 mm for LED 3.6. The radiometric map is acquired by the calibrated IR camera over an approximate 5 x 5 deg square field-of-view (FOV). The broad spectral pass band of the calibrated camera fully integrates the irradiance spectrum of the LED. The spatial distribution is fairly uniform with some low frequency spatial structure and noticeable roll-off at the edges. The other LEDs under test exhibit spatial irradiance maps of similar uniformity.

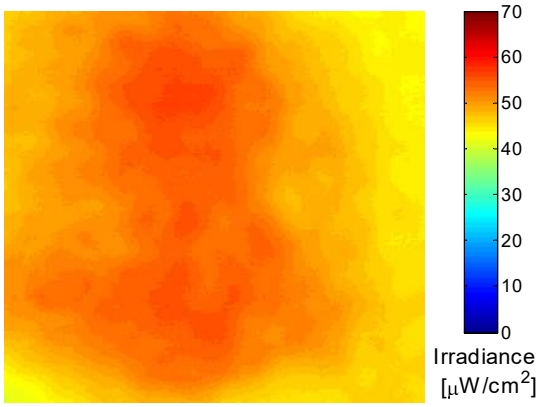

Figure 2. Spatial irradiance map over 5 x 5 deg FOV for lensed LED 3.6 at 92 mm distance operating at 130 K.

A typical angular intensity distribution for the lensed LEDs is shown in Figure 3. The curve is normalized to a value of 1.0 at normal exitance (0 deg). The intensity is measured by mounting the source on a rotation stage and sampling the intensity with a small point detector. The shape of the intensity distribution is dictated by the lens and may be unacceptable for some applications.

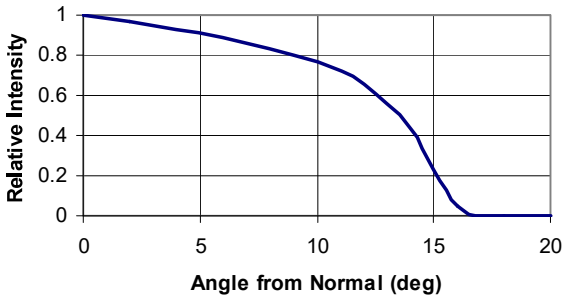

Figure 3. Typical intensity vs. exitance angle at 130 K.

Long term stability characteristics are measured by monitoring the radiometric output of an LED over 6 hours. Data is collected with an IR point detector at a sampling rate of 10 Hz. The detector and LED temperatures are controlled to better than 0.15 K over the full data collection period. Figure 4 plots the detector signal, normalized to a value of 1.000 at the start of the acquisition, versus time. Each point on the curve (red star) represents the average detector signal over a 6 minute interval, while the blue error bars represent the standard deviation of the samples within the same 6 minute window. The data shows that the LED is stable to approximately 1.0% peak-to-valley over the full 6 hour test window.

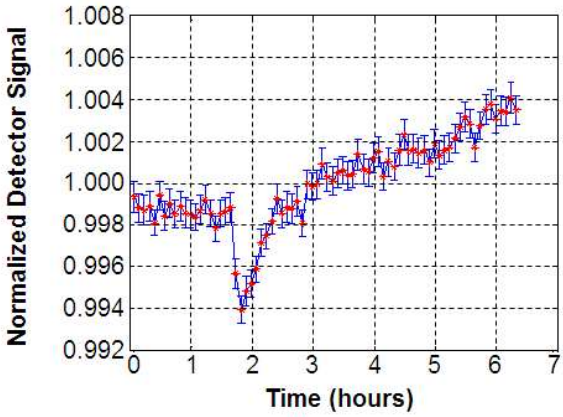

Figure 4. LED stability over 6 hours of operation at constant 130 K temperature.

Finally, the LED lens and packaging integrity is inspected via digital photography and microscopy before and after cryogenic cycling. A sample LED is quenched more than 10 times in liquid nitrogen from room temperature. Figure 5 shows the same LED before and after thermal cycling. No deformations or cracking of the lens or packaging was observed visually or in any subsequently collected data.

Figure 5. LED with lens before (left) and after (right) more than 10 cryogenic thermal cycles showing no lens damage.

4.2 Phase Two Results

For the second phase of the project, changes in the spectral, spatial, and radiometric characteristics of the IR LEDs are evaluated as a function of TID radiation exposure. For this phase, only LEDs 3.4, 3.6, and 3.8 are tested. Spectral, spatial, and radiometric measurements are acquired in relative units using the scanning monochromator and the IR camera with a precision of approximately 5% (1σ).

Table 6 summarizes the radiation testing schedule. Both LED 3.4 and LED 3.6 are exposed in 25 krad(Si) increments up to 100 krad(Si) total while LED 3.8 is exposed in smaller 5 krad(Si) increments up to 55 krad(Si) total. Only LED 3.4 exhibits any appreciable degradation in performance due to radiation exposure.

Table 6. Summary of Phase 2 LED Radiation Testing.

LED Unit Under Test	3.4 µm	3.6 µm	3.8 µm
Total Dose (krad(Si))	100	100	55
Dose Increment (krad(Si))	25	25	5
Number of Irradiations	4	4	11
Significantly Degraded Performance?	Yes	No	No

LED 3.4 shows significant degradation with radiation exposure. Figure 6 displays relative spatial distributions acquired at each exposure level. The images are each normalized to values between 0 and 1 and are presented with the pseudo-color scale shown. The images are acquired with identical viewing geometries so the large differences in the spatial distributions are due to radiation induced changes. Figure 7 plots normalized spectral irradiance vs. wavelength as a function of metered dose. The curves show severe changes in the spectral distributions, including wavelength shifts, spectral skew, and deviation from a Gaussian shape. LED 3.4 also experiences a significant reduction in radiometric output. Figure 8 plots the change in brightness with radiation exposure showing more than an 80% reduction at 100 krad(Si). The lower brightness is attributed to reduced QE since the input electrical power did not change with radiation exposure. LED 3.4 is very sensitive to radiation exposure and is not a suitable space calibration source.

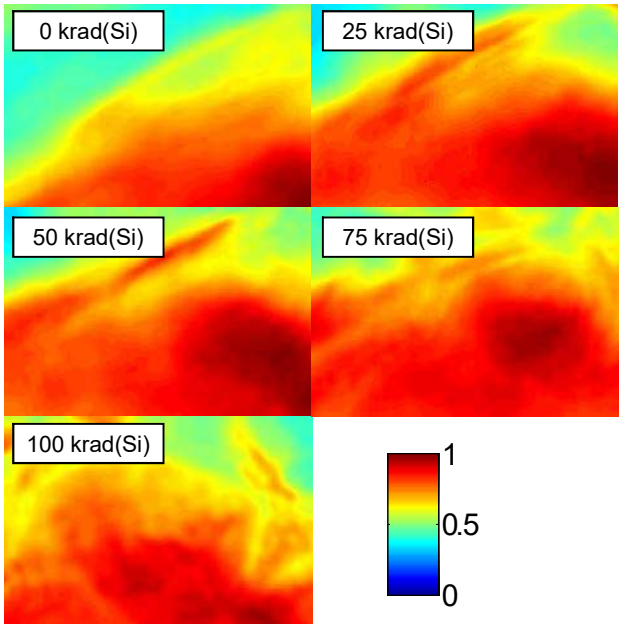

Figure 6. LED 3.4 spatial distributions vs. metered dose.

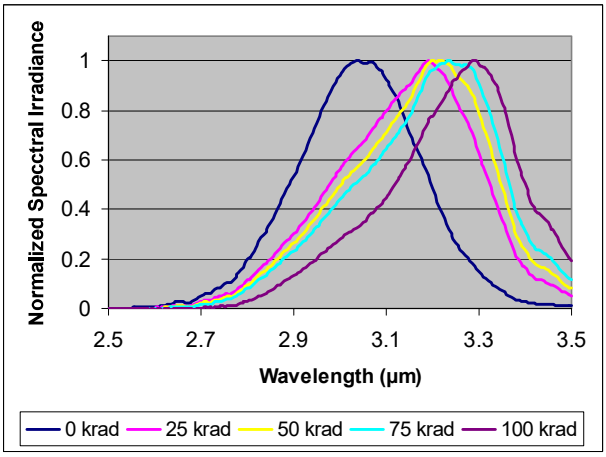

Figure 7: LED 3.4 spectral irradiance vs. metered dose.

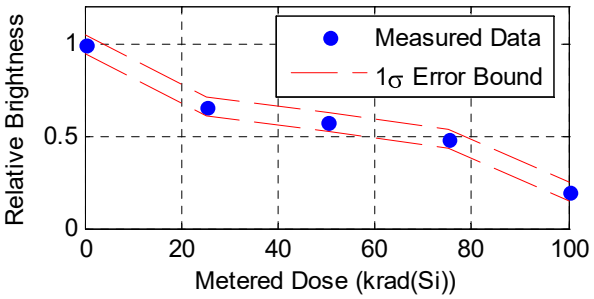

Figure 8. LED 3.4 relative brightness vs. metered dose.

Unlike LED 3.4, LEDs 3.6 and 3.8 do not exhibit significant performance degradation due to radiation exposure. The normalized spectral irradiance distributions for LEDs 3.6 and 3.8 (Figure 9 and Figure 10) show very few changes with radiation exposure. A small difference in shape is observed for LED 3.6 (note the left edge), but may be attributed to a slight change in operating temperature between exposures.

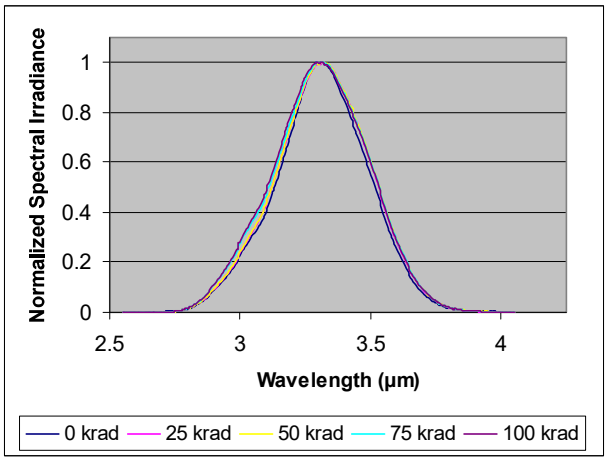

Figure 9. LED 3.6 spectral irradiance vs. metered dose.

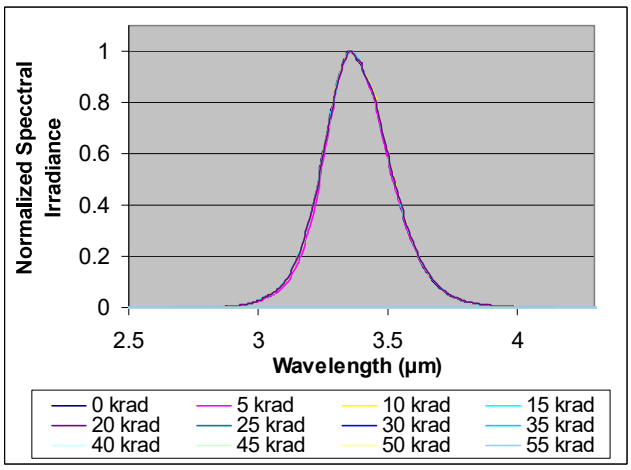

Figure 10. LED 3.8 spectral irradiance vs. metered dose.

Neither LED 3.6 nor 3.8 shows any reduction in radiometric output beyond measurement precision (Figure 11 and Figure 12) over the full range of radiation exposure levels. Finally, the spatial distributions for LED 3.6 and 3.8 remain constant to within measurement accuracy (Figure 13 and Figure 14). Both LEDs appear to be suitable calibration sources in space-based applications.

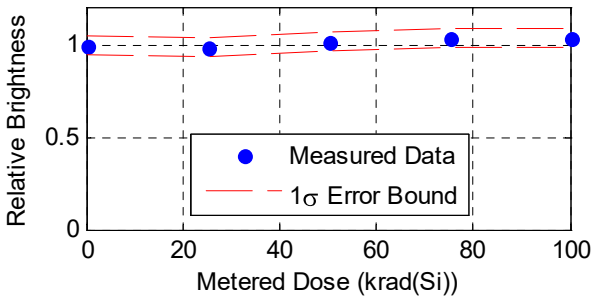

Figure 11. LED 3.6 relative brightness vs. metered dose.

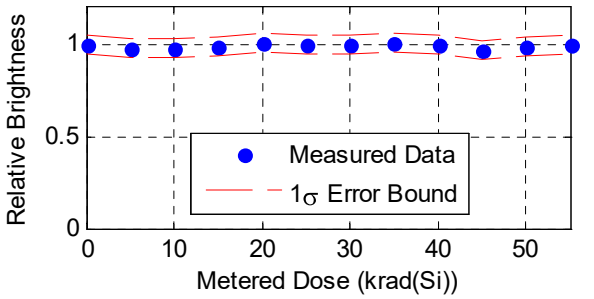

Figure 12. LED 3.8 relative brightness vs. metered dose.

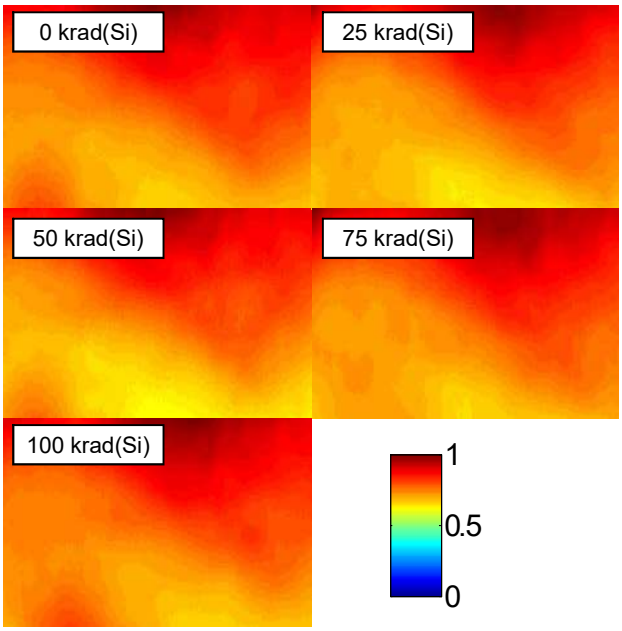

Figure 13. LED 3.6 spatial distributions vs. metered dose.

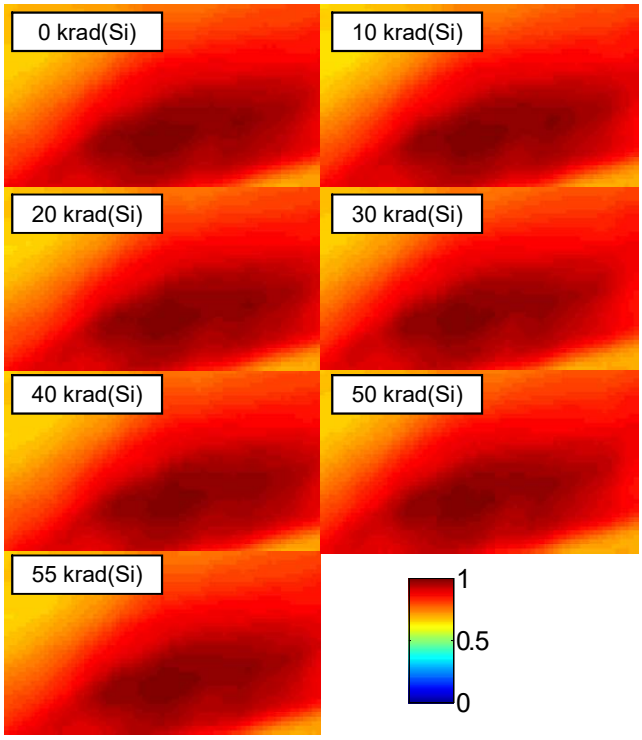

Figure 14. LED 3.8 spatial distributions vs. metered dose. Images at 5, 15, 25, 35, and 45 krad(Si) have been omitted.

5 Conclusions

Testing shows that certain IR LEDs are well suited for on-orbit calibration sources in space applications based on their spectral, spatial, radiometric, and environmental performance. A set of LEDs were characterized over a cryogenic operating temperature range between 130 and 150 K. Data shows that at cryogenic temperatures the diodes are up to 20 times more efficient, emit light at shorter wavelengths within a narrower spectral bandwidth, and only require approximately 60% more input electrical power. The spectral irradiance distributions are well approximated by Gaussian functions, and the LEDs provide spatially uniform irradiance with a radiometrically stable output over many continuous hours of operation. Precise temperature control is a likely requirement to maintain spectral and radiometric composition during calibration.

Radiation testing shows that only one LED exhibited significant changes when exposed to radiation, while no statistically significant changes were measured in the other two tested units. It is believed that different radiation sensitivities are due to the unique chemical composition and doping structures of each diode. Based on their optical and environmental characteristics, light emitting diodes are likely to be useful as calibration sources on future IR sensors in space applications.

Acknowledgment

The authors would like to acknowledge and thank our colleagues from the Innovation, Precision Mechanisms, Radiation, and Scatter Labs at Raytheon Space and Airborne Systems in El Segundo, California for their assistance with parts, repairs, and analyses. In addition, we thank Tom Chrien, Paul Randall, Chris Chovit, Eric Moskun, and Brandon Wilson for their contributions to our research.

References

[1] A. Milton, F. Barone and M. Kruer, "Influence of nonuniformity on IR focal plane array performance," *Optical Engineering*, Vol. 24, pp. 855-862, 1985.

[2] D. Starikov, I. Berichev, N. Medelci, E. Kim, Y. Wang and A. Bensaoula, "A hot electrons-based wide spectrum on-orbit optical calibration source," Proc. Space Technology and Applications International Forum, AIP Conf. Proceedings, Vol. 420, pp. 648-653, 1998.

[3] J. Nieke, M. Solbrig, K.H. Sumnich, G. Zimmermann and H.P. Roser, "Spaceborne spectrometer calibration with LEDs," SPIE 45th Annual Meeting – Earth Observing Systems V, Vol. 4135, San Diego, CA, 2000.